Discussion of "Laboratory Study on 3D Flow Structures Induced by Zero-Height Side Weir and Implications for 1D Modeling" by Giovanni Michelazzo, Hocine Oumeraci, and Enio Paris

DOI: 10.1061/(ASCE)HY.1943-7900.0001027

I. Rifai[1]; S. Erpicum[2]; P. Archambeau[3]; D. Violeau[4]; M. Pirotton[5]; K. El Kadi Abderrezzak[6]; and B. Dewals[7]

[1]Ph.D. Student, Dept. of ArGEnCo, Research Group Hydraulics in Environmental and Civil Engineering, Univ. of Liège, Quartier Polytech 1, Allée de la Découverte 9, B52/3+1, 4000 Liège, Belgique; EDF R&D, National Laboratory for Hydraulics and Environment, Saint Venant Laboratory for Hydraulics, 6 Quai Watier, BP 49, 78401 Chatou, France (corresponding author). ORCID: http://orcid.org/0000-0002-5554-3219. E-mail: i.rifai@doct.ulg.ac.be

[2]Assistant Professor, Dept. of ArGEnCo, Research Group Hydraulics in Environmental and Civil Engineering, Univ. of Liège, Quartier Polytech 1, Allée de la Découverte 9, B52/3+1, 4000 Liège, Belgique.

[3]Research Associate, Dept. of ArGEnCo, Research Group Hydraulics in Environmental and Civil Engineering, Univ. of Liège, Quartier Polytech 1, Allée de la Découverte 9, B52/3+1, 4000 Liège, Belgique.

[4]Senior Scientist, EDF R&D, National Laboratory for Hydraulics and Environment, Saint Venant Laboratory for Hydraulics, 6 Quai Watier, BP 49, 78401 Chatou, France.

[5]Professor, Dept. of ArGEnCo, Research Group Hydraulics in Environmental and Civil Engineering, Univ. of Liège, Quartier Polytech 1, Allée de la Découverte 9, B52/3+1, 4000 Liège, Belgique.

[6]Expert Researcher, EDF R&D, National Laboratory for Hydraulics and Environment, Saint Venant Laboratory for Hydraulics, 6 Quai Watier, BP 49, 78401 Chatou, France.

[7]Associate Professor, Dept. of ArGEnCo, Research Group Hydraulics in Environmental and Civil Engineering, Univ. of Liège, Quartier Polytech 1, Allée de la Découverte 9, B52/3+1, 4000 Liège, Belgique.

Introduction

The authors investigated the three-dimensional (3D) flow structures developing in the vicinity of a zero-height side weir. They conducted laboratory experiments under steady flow conditions in a 5.1-m-long, 0.30-m-wide glass-walled flume with a rectangular cross section and an adjustable side opening. Gravels were fixed on the main channel bottom to provide a realistic flow resistance. The downstream water level was controlled by a sluice gate located at the end of the flume. The sluice gate was set in order to ensure subcritical flow conditions in the main channel.

The paper provides a detailed description of the complex flow structures induced by a zero-height side weir and their implications for one-dimensional (1D) modeling of problems similar to those involving side weirs. The authors found that Borghei and colleagues' (1999) formula provides the best predictions for the side weir discharge. The discussers would like to comment on the validity of this formula considering also the experimental tests that involved flow regime changes and a hydraulic jump. On the other hand, the authors claimed that 55 to 60% is an upper bound for the ratio between the side discharge and the inflow discharge for subcritical flows. Herein, the discussers would like to emphasize that this limit depends strongly on the outflow boundary condition in the main channel. The notations used in this discussion are the same as those defined by the authors.

1D Numerical Simulations

The laboratory experiments performed by the authors have been simulated using the complete Saint-Venant equations, solved by a 1D finite volume model similar to that proposed by Kerger et al. (2011). Only the main channel was represented. The inflow discharge Q_u was set at 10 L/s. The main channel roughness was described through a Manning coefficient of 0.024 $s/m^{1/3}$. The downstream boundary condition was a rating curve interpolated from the experimental values obtained with a 2-cm-elevated sluice gate (Michelazzo 2014). The side opening discharge Q_s was calculated using Borghei and colleagues' (1999) formula for a zero-height side weir:

$$\frac{dQ_s}{dx} = \frac{2}{3} \cdot C_M \cdot \sqrt{2g \cdot h(x)^3} \tag{1}$$

where h = flow depth in front of the side weir (m); and C_M = coefficient (−) calculated as $C_M = 0.7 - 0.48\mathsf{F}_u + 0.06L_s^*$ with F_u the Froude number just upstream of the side weir and $L_s^* = L_s/B$.

In contrast with the authors' approach, the present numerical model simulates discontinuous flow profiles involving flow regime changes and hydraulic jumps. This enables the discussers to assess the performance of Borghei and colleagues' (1999) formula beyond the range of conditions considered by the authors.

Validity of the Borghei et al. (1999) Formula

The authors assessed the performance of the Borghei et al. (1999) formula for subcritical flows in the main channel. However, in the experimental runs B14, B15, and B16, a supercritical zone was present followed by a hydraulic jump (cf. Fig. 4 in the original manuscript). The discussers performed two series of numerical simulations covering all the experimental runs presented in the discussed paper (Fig. 1):

- In the first one, the discussers simply applied Borghei and colleagues' (1999) formula to calculate the discharge coefficient C_M from the Froude number F_u.
- In the second one, the discussers assumed that F_u may not be representative of the flow conditions downstream of the hydraulic jump. Therefore, the discussers slightly modified the Borghei et al. (1999) formula: the discussers updated the value of C_M downstream of the hydraulic jump using the Froude number

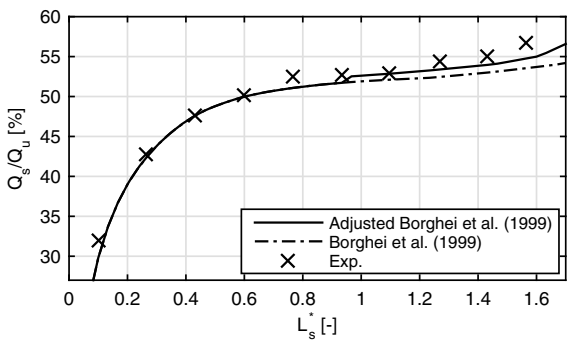

Fig. 1. Ratio of diverted discharge as a function of the dimensionless side weir length

F'_u calculated immediately downstream of the hydraulic jump (e.g., $F'_u/F_u \approx 0.7$ for $L^*_s = 1.6$).

The dashed line in Fig. 1 shows the side discharge computed by the 1D numerical model and the standard Borghei et al. (1999) formula. The results are in good agreement with the experimental data with an average error of 1.1 L/s. Deviations between the computed and experimental values are quite large for the shortest side weir only (i.e., $L^*_s = 0.1$). This may result from two reasons: (1) the Borghei et al. (1999) formula was derived from an experimental dataset in which L^*_s was varied in the range between 0.67 and 2.33, and (2) the downstream rating curve shows a high sensitivity for the highest water levels (cf. Fig. 4 in the original manuscript). For the configurations depicting flow regime changes (i.e., B14, B15, and B16), the standard Borghei et al. (1999) formula computes the lateral discharge with a relative error that is below 6%. Updating the estimate of C_M downstream of the hydraulic jump, the relative error is further reduced to 3.5% (solid line in Fig. 1). This confirms that slightly adapting the coefficient C_M in Borghei and colleagues' (1999) formula in the presence of a hydraulic jump leads to improved computations of the side discharge. The small jump in the solid line in Fig. 1 ($L^*_s \approx 0.95$) corresponds to the occurrence of a flow regime change and the calculation of the coefficient C_M with the Froude number F'_u downstream of the hydraulic jump.

Downstream Boundary Condition

The authors carried out the experiments using a sluice gate downstream of the main channel, which is relatively standard in similar laboratory studies on side weirs (Borghei et al. 1999; Emiroglu et al. 2011; Rahimpour et al. 2011). In their conclusions, the authors stated "An asymptotic limit of the ratio Q_s/Q_u was supposed to exist around a value of 55–60%, at least for the tested subcritical conditions." Nevertheless, it should be highlighted that this value is highly dependent on the downstream boundary condition and the given value is specific, not to the subcritical flow regime, but to the particular setting of the sluice gate used in the experiment. Indeed, testing other downstream boundary conditions leads to different diverted discharge ratios.

The discussers have tested three additional rating curves for the downstream boundary in the 1D numerical model, corresponding respectively to (1) a rectilinear weir with a 9.7-cm-high 30-cm-wide crest, (2) a 6.5-cm-high and 15-cm-wide rectangular notch, and (3) a triangular weir with an opening angle of 60°. These configurations were set to obtain the same lateral discharge for the first configuration of the side weir ($L^*_s = 0.1$). Results show that the three rating curves lead to different estimates of the lateral discharge as a function of the side weir lengths, even for subcritical flow regime cases (Fig. 2). The flow remains subcritical and the diverted ratio, Q_s/Q_u, reaches 100% for the rectilinear weir after the water level drops under the crest level, which corresponds to a side weir flow with a dead end (Hager and Volkart 1986; Hager 1987), 97% for the rectangular notch and 88% for the triangular weir.

The description of the 3D flow structures reported by the authors is also influenced by the downstream boundary condition. As reported by Hager and Volkart (1986) for subcritical flow conditions, the *flow separation zone* can even expand to the whole width of the main channel and a *backflow zone* forms in the case of a dead end. The main channel downstream velocities in the three additional cases are lower than those measured by the authors. Hence, the rectangular notch and triangular weir cases are expected to develop 3D flow structures of intermediate characteristics between the two typical configurations presented by Hager and Volkart (1986) and by the authors. Furthermore, the outflow angles can reach 90° at the downstream end of the side weir (Hager 1987), whilst the downstream outflow angle reported by Michelazzo (2014) decreases to 48° for the maximum side weir length ($L^*_s = 1.6$).

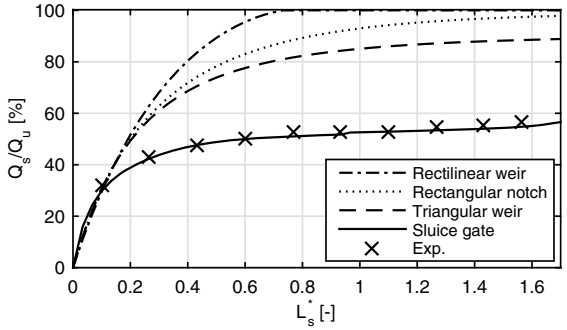

Fig. 2. Ratio of diverted discharge as a function of the dimensionless side weir length for different downstream weir alternatives

The choice of the flow regulating system at the downstream end has a strong influence on the evolution of the free surface profile, the diverted discharge, and the flow structures developing downstream of the side weir. This must be carefully accounted for in problems similar to those of side weirs, such as lateral dike breaching modeling, in which the water profiles, the velocity field, and the flow structures in the near field of the breach influence the erosion processes and consequently the dynamics of the breach evolution.

References

Borghei, S. M., Jalili, M. R., and Ghodsian, M. (1999). "Discharge coefficient for sharp-crested side weir in subcritical flow." *J. Hydraul. Eng.*, 10.1061/(ASCE)0733-9429(1999)125:10(1051), 1051–1056.

Emiroglu, M. E., Agaccioglu, H., and Kaya, N. (2011). "Discharging capacity of rectangular side weirs in straight open channels." *Flow Measure. Instrum.*, 22(4), 319–330.

Hager, W. H. (1987). "Lateral outflow over side weirs." *J. Hydraul. Eng.*, 10.1061/(ASCE)0733-9429(1987)113:4(491), 491–504.

Hager, W. H., and Volkart, P. U. (1986). "Distribution channels." *J. Hydraul. Eng.*, 10.1061/(ASCE)0733-9429(1986)112:10(935), 935–952.

Kerger, F., Archambeau, P., Erpicum, S., Dewals, B. J., and Pirotton, M. (2011). "A fast universal solver for 1D continuous and discontinuous steady flows in rivers and pipes." *Int. J. Numer. Methods Fluids*, 66(1), 38–48.

Michelazzo, G. (2014). "Breaching of river levees: Analytical flow modelling and experimental hydro-morphodynamic investigations." Ph.D. thesis, Faculty of Engineering, Univ. of Florence, Florence, Italy.

Rahimpour, M., Keshavarz, Z., and Ahmadi, M. (2011). "Flow over trapezoidal side weir." *Flow Measure. Instrum.*, 22(6), 507–510.